Performance Estimation of UTC and Several UTC(k) Realizations During the Past 25 Years

C. A. Ortiz, E. de Carlos-López, A. Medina-Herrera, Michael A. Lombardi, *Member, IEEE*, and J. M. López-Romero, *Member, IEEE*

***Abstract*— This article analyzes data published by the Bureau International des Poids et Mesures (BIPM) over the past 25 years to assess the long-term performance of the Coordinated Universal Time (UTC) timescale and ten other physical realizations of UTC. We utilize a combination of the three-cornered hat method and dynamic Allan deviation estimation to provide a comprehensive evaluation of UTC performance over such an extended period of time. Furthermore, we present a forecast of UTC's performance for the next ten years. We highlight key events based on data published by the time department of the BIPM during the period from January 1998 to December 2023. We determine that UTC instability, for averaging periods (τ) of five days and one year, has decreased by an order of magnitude in respective periods of 18.9 years and 16.9 years, respectively. If this improvement continues during the next decade, we estimate that the instability of UTC will decrease to 7.8×10^{-17} for $\tau = 5$ days and 1.1×10^{-17} for $\tau = 1$ year. We discuss the correlation between the development of primary and optical frequency standards, the improvement in time transfer methods, and the performance of the UTC(k) timescales.**

***Index Terms*— Instability, timescale, time transfer, Coordinated Universal Time (UTC), UTC(k).**

I. Introduction

The development of quantum physics provided the foundation for the invention of atomic clocks, which first appeared in the late 1940s. The current definition of the SI second, the base unit of time, was established at the 13th General Conference on Weights and Measures (CGPM) in 1967 as the duration of 9, 192, 631, 770 periods of the electromagnetic radiation associated with the transition between the two hyperfine levels of the ground state of the ^{133}Cs atom at 0 K [1], [2]. The performance of primary frequency standards has improved at a rate of about one order of magnitude per decade during the past 50 years. However, during the past 20 years, the performance of optical atomic clocks has improved at an even faster rate, with an astonishing average rate of almost three orders of magnitude per decade.

The Bureau International des Poids et Mesures (BIPM) in Sèvres, France, receives regular data contributions from about 80 international timing laboratories [3], [4]. These data are used to calculate several atomic timescales, including the Free Atomic Time (EAL), International Atomic Time (TAI), and Coordinated Universal Time (UTC).

UTC is the international reference that forms the basis for all measurements of time and frequency made worldwide. The formation of UTC is accomplished in three steps. The first step is to compute EAL, the free running atomic timescale. EAL is a timescale based solely on the measurements of atomic clocks that has an epoch of January 1, 1958. The timescale TAI is formed by making small frequency corrections to EAL, obtained from the measurements of the primary frequency standards operated by about ten national metrology institutes (NMIs). The frequency of UTC is equivalent to TAI, but unlike TAI, UTC is adjusted so that it stays within ±0.9 s of the astronomical timescale UT1, which is based on the rotational rate of the Earth. TAI is not adjusted to agree with UT1, and, therefore, the time difference between UTC and TAI, expressed in integer seconds, represents the divergence between atomic time and astronomical time since January 1, 1958 [5], [6], [7], [8]. The following equations define the UTC timescale:

$$\mathrm{UTC} = \mathrm{TAI} + n \tag{1}$$

where n is an integer number of seconds and

$$|\mathrm{UTC} - \mathrm{UT1}| \leq 0.9 \text{ s}. \tag{2}$$

UTC is produced by calculations and, therefore, does not produce the physical time and frequency signals that are needed for practical applications. The necessary physical signals are produced by local realizations of UTC, called UTC(k), with the label k indicating the name of the laboratory that maintains the timescale. The laboratory is required to have at least one atomic clock, but the most stable and accurate UTC(k) timescales include multiple atomic clocks that are continuously measured and intercompared. The UTC(k) and individual clock measurements are sent to the BIPM and included in the UTC calculation.

Received 23 October 2024; revised 31 January 2025; accepted 10 February 2025. Date of publication 14 March 2025; date of current version 2 April 2025. The Associate Editor coordinating the review process was Dr. Marco Agustoni. *(Corresponding author: J. M. López-Romero.)*

C. A. Ortiz and E. de Carlos-López are with the Centro Nacional de Metrología (CENAM), Santiago de Querétaro 76246, México (e-mail: cortiz@cenam.mx; edlopez@cenam.mx).

A. Medina-Herrera is with the Physikalisch-Technische Bundesanstalt (PTB), 10587 Berlin, Germany, and also with Centro de Investigación y de Estudios Avanzados del IPN (CINVESTAV), Unidad Querétaro, Santiago de Querétaro 76230, México (e-mail: andres.medina-herrera@ptb.de).

Michael A. Lombardi, retired, was with the National Institute of Standards and Technology (NIST), Boulder, CO 80305 USA. He resides in Broomfield, CO 80023 USA (e-mail: michael.lombardi@nist.gov).

J. M. López-Romero is with the Centro de Investigación y de Estudios Avanzados del IPN (CINVESTAV-IPN), Unidad Querétaro, Santiago de Querétaro 76230, México (e-mail: jm.lopez@cinvestav.mx).

Digital Object Identifier 10.1109/TIM.2025.3551463

The UTC–UTC(k) time differences are recorded at five-day intervals and published in the monthly BIPM Circular T document [9]. The laboratories that maintain the UTC(k) timescales reside in nations that are signatories of the International Committee for Weights and Measures mutual recognition arrangement (CIPM MRA) [10], [11] and the Circular T provides the results of the BIPM's key time comparison, called CCTF-K001.UTC [12].

The physical realizations of UTC that the key comparison participants provide are very important for a variety of industrial systems and applications that require a stable and accurate source of time. Some examples are telecommunications systems [13], [14], global navigation satellite systems (GNSS) [15], [16], defense systems [17], electrical power distribution systems, and many others. Signals originating from UTC(k) timescales are distributed by different means, including GPS common view and all-in-view methods [18], [19], two-way time and frequency transfer methods [20], [21], terrestrial radio signals [22], local and wide-area networks using protocols such as the precise time protocol (PTP) [23], [24] and network time protocol (NTP) [25], [26], and by ordinary telephone lines.

In Section II, we present time differences of ten UTC(k) timescales with respect to UTC for the period from the Modified Julian Date (MJD) 50800 (December 8, 1997) to the MJD 60309 (December 31, 2023), analyzing some key events that influenced their performance (stability and accuracy). In Section III, the 25-year performance of UTC using the three-corner hat method is analyzed. In addition, the participation of atomic clocks and primary and secondary standards in the formation of UTC is presented. We conclude by discussing the future evolution of UTC and UTC(k) timescales.

II. Some UTC(k) Timescales and Their Performance

In this section, we analyze the performance of ten UTC(k) timescales, beginning with some general comments. We then note key events that are related to the generation and performance of specific timescales (e.g., the contributions of a primary frequency standard). We also present dates when remarkable advancements in the stability and accuracy of a timescale have occurred, correlating these dates with improvements implemented in the laboratories.

The ten UTC(k) timescales included in our analysis are UTC(USNO), UTC(NIST), UTC(PTB), UTC(OP), UTC(ROA), UTC(NPL), UTC(KRIS), UTC(IT), UTC(CNM), and UTC(ORB). The identifier USNO refers to the United States Naval Observatory, NIST refers to the National Institute of Standards and Technology of the United States of America, PTB refers to the *Physikalish Technische Bundesanstalt* of Germany, OP refers to the Paris Observatory of France, ROA refers to the *Real Observatorio de la Armada* of Spain, NPL refers to the National Physical Laboratory of England, KRIS refers to the Korea Research Institute of Standards and Science of the Republic of Korea, IT refers to the *Istituto Nazionale di Ricerca Metrologica* of Italy, CNM refers to the *Centro Nacional de Metrología* of Mexico, and ORB refers to the Royal Observatory of Belgium.

Fig. 1 shows the UTC–UTC(k) time differences for the 10 laboratories, using data published in the BIPM Circular T documents, for the period from MJD 50800 to MJD 60309 (January 1998–December 2023).

For UTC(NIST), two key events can be observed in which the timescale performance changes are highlighted with pink arrows in Fig. 1(a). The first event occurred near MJD 52200 (October 18, 2001) and second occurred around MJD 57500 (April 22, 2016). The first event involved a modification in the UTC(NIST) timescale algorithm, which was formerly designed to minimize frequency stability at the expense of time accuracy. The algorithm was fine-tuned in 2001 to simultaneously maintain both characteristics of a good timescale, frequency stability, and time accuracy [27]. The second event in 2016 involved the weekly steering of UTC(NIST) that was made possible by the BIPM's publication of Rapid UTC (UTCr) [28].

During the last 25 years, several primary frequency standards (cesium fountain clocks), were developed by the NIST Time and Frequency Division [29], [30]. Interestingly, there was not a direct correlation between primary frequency standards development at NIST and UTC(NIST) performance. The first NIST cesium fountain clock was developed in 1998 [31], [32], [33], and the accuracy of the second cesium fountain was evaluated around 2014 [34], [35]. However, UTC(NIST) performance remained unchanged until 2016 [36]. It is important to note that UTC(NIST) is not always steered to NIST cesium fountain clocks.

On MJD 55228 (February 1 2010), UTC(PTB) timescale was realized using an active hydrogen maser (AHM) steered in frequency via a phase microstepper, with an algorithm that utilizes frequency comparison data obtained from measurements of AHM and the primary and commercial cesium clocks of PTB [37], [38]. Due to that action, the time stability of UTC(PTB) improved by about an order of magnitude when averaged several months or longer. It is interesting to note that the operation of the PTB CSF1 cesium fountain clock began around June 2000 [39], [40], however, it was not used to steer UTC(PTB) until 16 years later. PTB developed a second cesium fountain clock, CSF2, around 2006 [41]. Between 2006 and 2008, a series of technical enhancements were introduced, such as state selection, improved Ramsey fringe contrast, and lower atomic cloud temperature. Since December 2008, the frequency uncertainty of the clock has been evaluated, and multiple comparisons with CSF1 have been carried out [41], [42]. During 2017–2018, the two cesium fountain clocks operated almost 100 % of the time, and UTC(PTB) was composed of these fountain clocks and an AHM and was gently steered to UTC to obtain long-term time accuracy [37]. However, no immediate impact on UTC(PTB) performance was observed. Finally, we highlight that, to the best of our knowledge, UTC(PTB) was the first UTC(k) that included a continuously running cesium fountain clock.

At Sytèmes de Référence Temps Espace (SYRTE), three cesium fountain clocks were developed, named FO1, FOM, and FO2. FO1 was developed around 1995 [43]. The second fountain clock, the FOM, was a prototype for the Projet d'horloge atomique par refroidissement d'atomes en orbite (PHARAO) cold atom space clock [44] and was later modified to be a transportable fountain clock. FO2 is a dual ^{133}Cs/^{87}Rb fountain clock put into operation in 2010 [45]. Beginning 2013, the three fountain clocks were used to steer the UTC(OP). On MJD 56229 (October 29, 2012), a new realization of UTC(OP) was introduced. This version relied on steering an AHM, controlled by the SYRTE atomic fountains using a frequency offset generator. The result of this steering is an excellent improvement in UTC(OP) performance, as can be appreciated in Fig. 1(c) [46].

Two noteworthy events affected UTC(ROA). The first one happened around MJD 55000 (June 18, 2009) [47], and the second occurred around MJD 58124 (July 1, 2018). UTC(ROA) was generated until MJD 55 000 using the output signal of a commercial high-performance cesium beam atomic clock. After that date, the timescale was produced using an AHM. On MJD 55927 (January 1, 2012), ROA began using the UTCr timescale to adjust UTC(ROA) [48]. Around MJD 58124, a new ROA facility with Faraday shielding was used to house the ensemble of atomic clocks in charge of the UTC(ROA) production. The clocks in the new facility are situated over an anti-vibration platform, and temperature oscillations can be controlled to within 0.1 K per day.

NPL developed three cesium fountain clocks, NPL-CsF1 in 2005 [49], [50], NPL-CsF2 in 2010 [51], [52], and NPL-CsF3 in 2016 [53]. Until 2017, the performance UTC(NPL) was not influenced by the development of primary frequency standards at the NPL. As shown in Fig. 1(e), the frequency stability and time accuracy of the UTC(NPL) remained nearly unchanged from MJD 50800 (December 18, 1997) until around MJD 57800 (February 16, 2017). However, beginning MJD 58000 (September 4, 2017), UTC(NPL) showed a significant improvement in its frequency stability and time accuracy, which can be attributed to steering adjustments involving both NPL-CsF2 and NPL-CsF3 [54].

Two key events can be observed that influenced UTC(KRIS) performance. One occurred around 2003 when the peak-to-peak values of UTC–UTC(KRIS) time differences became systematically smaller than 100 ns when more frequent corrections were applied to UTC(KRIS). From MJD 53800 (March 6, 2006) to MJD 55800 (August 27, 2011), the frequency stability of UTC(KRIS) was not optimal when averaged for a few months. This was corrected when an AHM was used to produce UTC(KRIS), along with an improved GPS Carrier Phase (CP) time transfer links to the BIPM [55], resulting in improvements in both frequency stability and time accuracy.

Two events influenced UTC(IT) performance. The first event occurred on MJD 53900 (June 14, 2006); up to that date UTC(IT) had been generated by a single commercial cesium beam frequency standard. From that date forward, UTC(IT) was generated by an AHM [56], and later, a second event occurred about MJD 56600 (November 04, 2013) steering three AHMs with different criteria improving the stability. The first criterion was based on BIPM's UTCr data, the second was based on an ensemble of six commercial cesium beam clocks and four AHMs. The third criterion was based on measurements of the cesium fountain clock name ITCsF2 [57], [58], [59] that uses a cryogenically cooled flight region to minimize the blackbody radiation (BBR) effect [60]. The ITCsF2 clock is an improvement of the earlier atomic fountain named (IEN CsF1) [61].

Three remarkable events occurred that impacted UTC(CNM). The first took place around MJD 54480 (January 15, 2008) when the Sistema Interamericano de Metrología (SIM) Timescale (SIMT) [62] was used to compare UTC(CNM) in almost real time, preceding the UTCr appearance. Then, around MJD 55100 (September 26, 2009), a timescale based on an ensemble of industrial cesium clocks, an AHM, and a high-resolution phase and frequency offset generator was implemented [63]. Finally, around MJD 57204 (July 1, 2015), a new timescale algorithm was implemented to compensate for short-term noise.

The UTC(ORB) laboratory was moved to a new temperature-stabilized facility on MJD 52334 (March 1 2002), resulting in a significant improvement in frequency stability [64]. As shown in Fig. 1(i), it can be observed that around MJD 53000 (December 2003), the frequency stability of UTC(ORB) improved in the short term. During the period from MJD 53371 (January 1 2005) to MJD 54466 (January 1 2008), UTC(ORB) maintained three commercial cesium beam clocks and two AHMs. UTC(ORB) was then generated from the output frequency of an AHM, with auto-tuning performed using the second AHM [65]. Currently, UTC(ORB) continues to use the signal from one of the AHMs, with its frequency automatically tuned to maintain stability with UTC. Furthermore, the control of UTC(ORB) involves regular comparisons with all other clocks, including their average, and ongoing comparisons are made with UTC(USNO) using the GPS common view technique [66].

The USNO operates a Master Clock (MC), which serves as the primary reference for UTC(USNO). From MJD 51179 (January 1, 1999) to the end of 2012, UTC(USNO) was generated using an ensemble of 73 industrial cesium clocks and 21 AHMs, maintaining a difference of approximately 5 ns root mean square (rms) with respect to UTC [67]. Around MJD 54739 (September 30, 2008), the USNO introduced new facilities with a temperature stability of 0.1 K and 3 % relative humidity. In addition, two rubidium fountains were designed to operate continuously, and new timescale algorithms incorporated the superior performance of the atomic fountains. These enhancements significantly contributed to the improved frequency stability of UTC(USNO) [65]. Fig. 1(j) shows the stability of UTC(USNO) after using UTCr data to apply more rapid corrections [68].

The international timekeeping community has reduced the UTC–UTC(k) time differences by one order of magnitude or more during the last 25 years. This improvement rate is, on average, similar to the historical rate of improvement in the accuracy of primary frequency standards. However, as we discuss later, it is important to note that there is no immediate correlation between the accuracy of the primary frequency standards and the stability of the timescale.

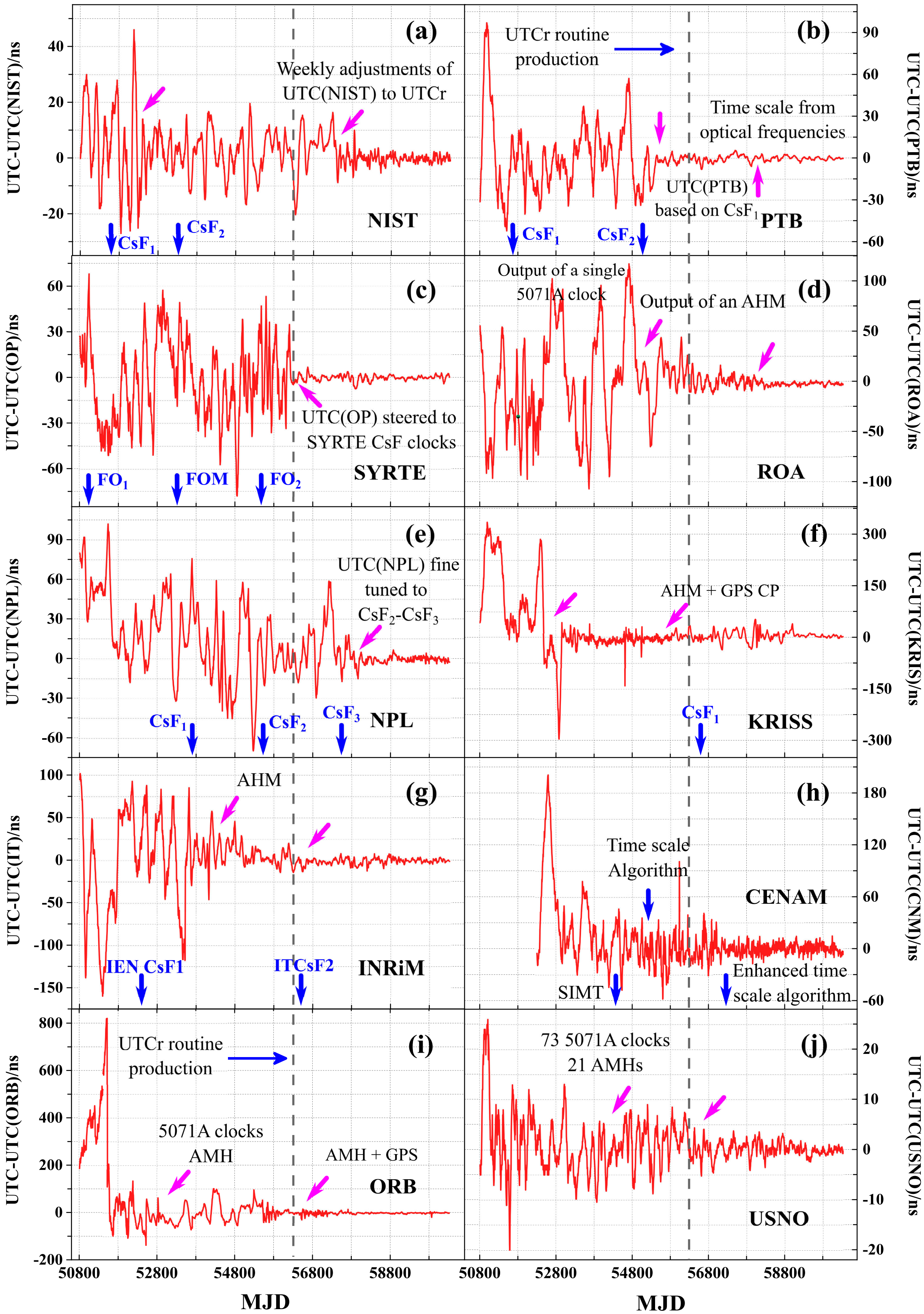

Fig. 1. Time differences of UTC and 10 local realizations of UTC(k), from MJD 50800 (January 1, 1998) to MJD 60309 (December 31, 2023). (a) UTC(NIST). (b) UTC(PTB). (c) UTC(OP). (d) UTC(ROA). (e) UTC(NPL). (f) UTC(KRIS). (g) UTC(IT). (h) UTC(CNM). (i) UTC(ORB). (j) UTC(USNO).

The dynamic Allan deviation [69] is an appropriate tool for analyzing the evolution of the UTC(k) scales and for better understanding their instability. This approach allows for the objective identification of the distinct stages or events that define each UTC(k) timescale. Fig. 2 shows the graphs of the dynamic Allan deviation corresponding to the different UTC–UTC(k) comparisons. The computation used one-year datasets consisting of 73 Circular T data points, one data point every five days, and shifted the entire dataset by one data point at a time. By varying the number of points in the datasets, the

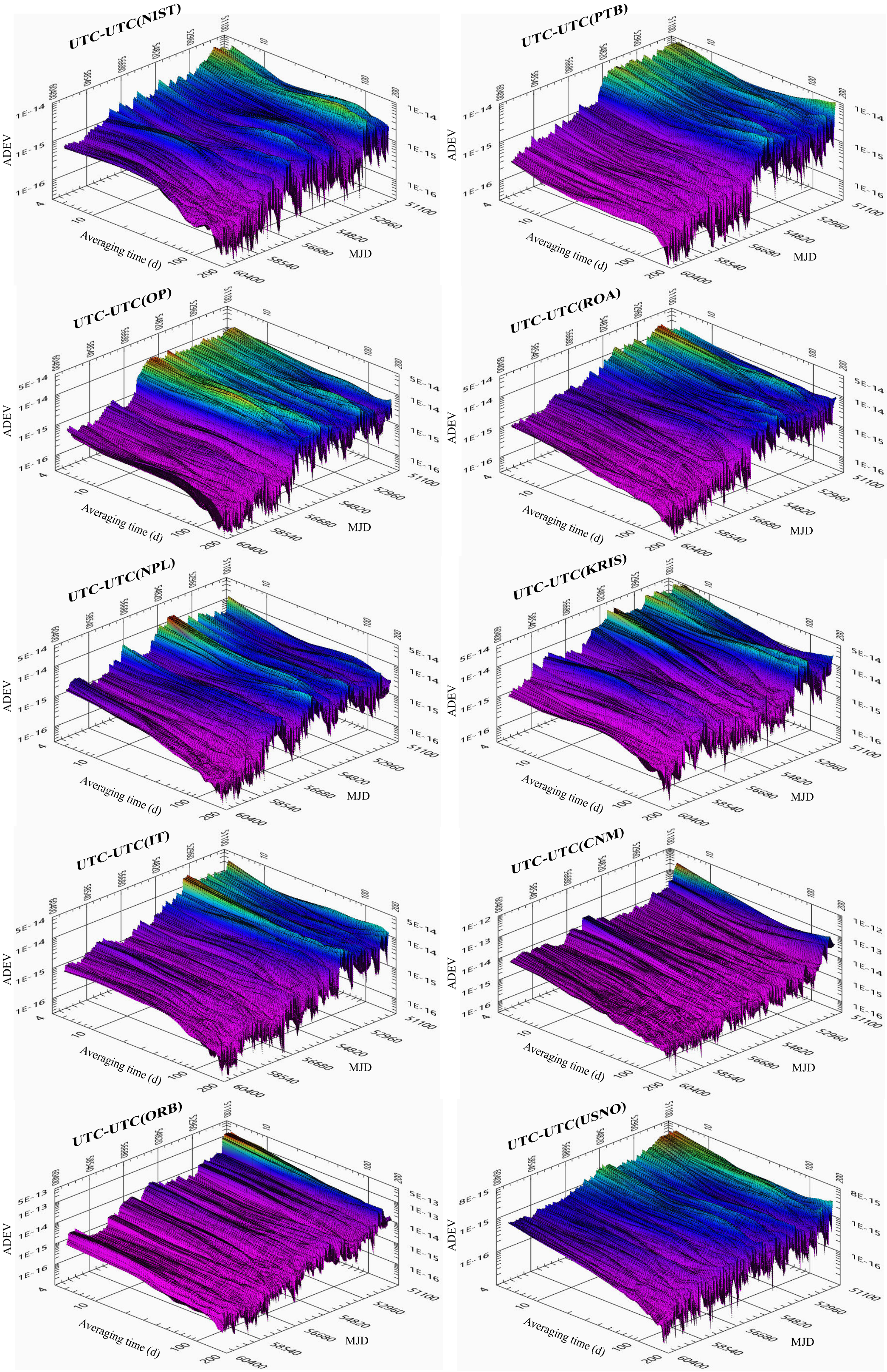

Fig. 2. Graphs of the dynamic Allan deviation of the different UTC–UTC(k) comparisons corresponding to the measurements in Fig. 1.

surface of the graphs can, of course, become smoother or less smooth, hiding or showing details visible in the short term. Using a one-year dataset provides enough resolution to see the changes that occur from year to year, but also provides statistical results that have an acceptable confidence level.

III. UTC Performance

As previously mentioned, the formation of EAL is the first step in the formation of UTC. EAL is formed using a weighted average of the AHMs and cesium atomic clocks that are located at the UTC(k) laboratories. Between 1997 and 2013,

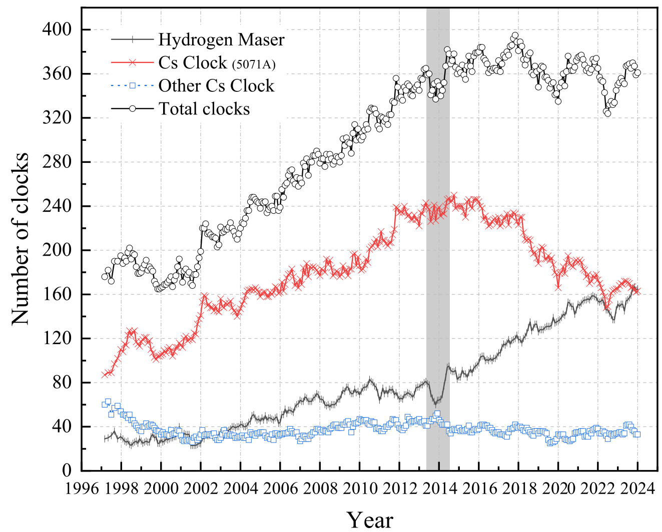

Fig. 3. Total number of clocks participating effectively (clocks with nonzero weights) in EAL according to information published by BIPM from January 1998 to December 2023 (https://webtai.bipm.org/ftp/pub/tai/other-products/stats/distribution.txt).

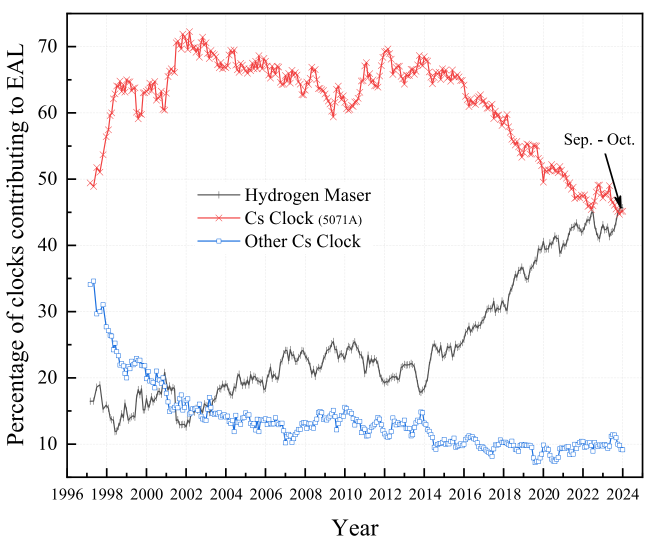

Fig. 4. Percentage of clocks participating effectively (clocks with nonzero weights) in EAL according to information published by BIPM from January 1998 to December 2023 (https://webtai.bipm.org/ftp/pub/tai/other-products/stats/distribution.txt).

the total number of clocks participating in EAL (with nonzero weights) increased almost linearly from approximately 180 to 350 clocks (see Fig. 3), reaching a maximum value of 395 in October 2017. The number subsequently dropped, reaching, 324 in 2022. However, the drop in the number of clocks has not compromised the performance of UTC because, among other reasons, the percentage of AHMs in the total clock population has increased from 20 % to more than 40 % (see Fig. 4). An AHM has short-term stability ($\tau < 7$ days) that is about 100× better than a commercial cesium beam clock, and its noise floor, reached in a period about 10 000× shorter, is about 5× to 10× lower.

The increase in the proportion of AHM is attributed to an update of the weighting algorithm in the 2014 [70] with a new frequency prediction algorithm [71], which introduced the quadratic model in phase data for the atomic clocks. This allowed the consideration of the frequency drift of the AHMs and the aging rate of cesium clocks, making the worldwide ensemble of atomic clocks more efficient. The weighting strategy applied in UTC considers the prediction used in calculating EAL and is based on the principle that a good clock is a stable and predictable clock. Since 2016, no commercial cesium beam clock has received maximum weight in the EAL calculation, which justifies the increased use of AHMs in UTC(k) laboratories. An AHM costs about 4× more than a cesium beam clock, but its life expectancy is about 4× longer. However, an AHM requires more demanding environmental control (temperature, pressure, EM, and mechanical isolation) and continuous telemetry monitoring to ensure the best metrological performance.

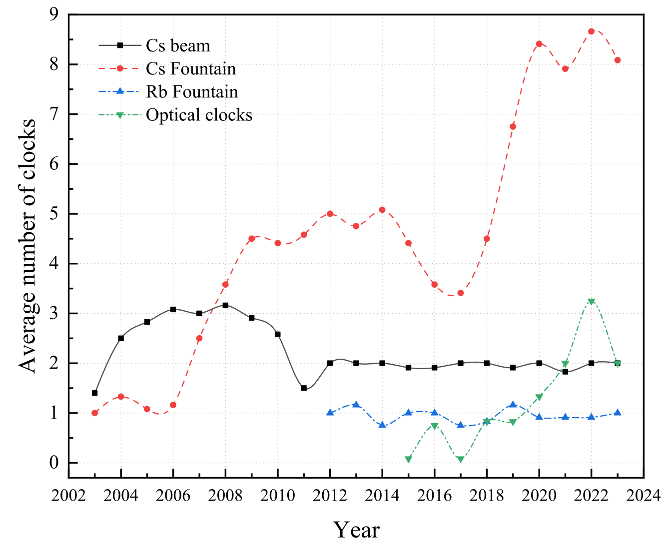

Fig. 5. Primary frequency standards and secondary representations of the second participating to TAI. Data obtained from https://webtai.bipm.org/database/show_psfs.html. Each point represents the average by year.

UTC has also benefited from improvements to TAI that are related to the improvements in the Primary and Secondary Frequency Standards (PFS/SFS), which steer TAI so that it maintains agreement with the definition of the International System (SI) second. The steering correction is determined by comparing the EAL frequency with that of the PFS/SFS. Based on information published by BIPM, Fig. 5 presents the evolution of PFS and SFS participating in the TAI production. The increase in the number of cesium fountain clocks and optical clocks has been notable since 2017. The coexistence of microwave and optical clocks is paving the way to an eventual redefinition of the SI second in terms of a unique optical transition, or a combination of optical transitions [72].

Finally, to complete the analysis of the 25 years performance of UTC, the three-corner hat method [73] was employed to assess the absolute dynamic instability of UTC. To do this, we used the Allan variance of UTC–UTC(k_i), UTC–UTC(k_j), and UTC(k_i)–UTC(k_j) differences, denoted as $\sigma^2_{y_i}$, $\sigma^2_{y_j}$, and $\sigma^2_{y_{ij}}$, respectively, for a given averaging time τ and MJD. As a first approximation, we assume that algebraic separation of individual variances is possible so that we can estimate the absolute instability of UTC, represented by $\sigma_{y_{\mathrm{UTC}}}$, as

$$\sigma^2_{y_{\mathrm{UTC}}} = \frac{1}{2}\left(\sigma^2_{y_i} + \sigma^2_{y_j} - \sigma^2_{y_{ij}}\right). \tag{3}$$

Data from the graphs featured in Fig. 2 were used to calculate the absolute instability of UTC along with (3). It is important to mention that for some combination of k_i, k_j, τ, and MJD, it is possible to obtain some invalid values ($\sigma^2_{y_{\mathrm{UTC}}} < 0$). To overcome this limitation, a simple average is calculated using different combinations of laboratories. Then, the simple average of the UTC Allan variance, using n laboratories is taken from all valid three-corner hats as

$$\langle\sigma^2_{y_{\mathrm{UTC}}}\rangle = \frac{2}{n(n-1)}\sum_{i=1}^{n-1}\sum_{j=i+1}^{n}\frac{1}{2}\left(\sigma^2_{y_i} + \sigma^2_{y_j} - \sigma^2_{y_{ij}}\right). \tag{4}$$

For a given number of laboratories n, it is possible to have $n(n-1)/2$ combinations of UTC–UTC(k_i), UTC–UTC(k_j), and UTC(k_i)–UTC(k_j) measurements to solve the three-corner hat. In each iteration, $n(n-1)/2$ values of $\sigma_{y_{\mathrm{UTC}}}$ are found, which are averaged. When the result of the three-corner hat in any of the possible combinations is invalid (negative variances), it is removed from the average. That is, if out of the $n(n-1)/2$ calculations x invalid values appear, the average is performed with $[n(n-1)/2]-x$ valid values. It should be noted that the multiple calculations of $\sigma_{y_{\mathrm{UTC}}}$, together with its average, enhance the UTC instability estimation and ensure that variances are positive.

Fig. 6 shows the simple average dynamic Allan deviation obtained with (4).

For Fig. 6, $n = 5$ laboratories were used to calculate the dynamic Allan deviation of UTC, that is, $n(n-1)/2 = 10$ calculations of $\sigma_{y_{\mathrm{UTC}}}$ were used to perform the averages in each iteration. The laboratories used to calculate the dynamic Allan deviation were NIST, NPL, OP, PTB, and USNO. These laboratories were chosen due to their lower percentage (approximately 40 %) of invalid data in the calculation of UTC instability.

To conclude this analysis and model the behavior of UTC instability over time, we make a base 10 exponential fit to the data of Fig. 6 in the MJD–ADEV plane. Then, the absolute instability of UTC for a given τ can be modeled as

$$\sigma_{y_{\mathrm{UTC}}}(\tau, t) \approx 10^{-\frac{t}{t_{10}(\tau)}}\sigma_{y_0}(\tau) \tag{5}$$

where σ_{y_0} is a function of the averaging time τ. t is the elapsed time since MJD 50814 (January 1, 1998) and $t_{10}(\tau)$ is the "tenth-life" time in which $\sigma_{y_{\mathrm{UTC}}}(\tau)$ decreases by one order of magnitude for the particular value of τ. This results in values of $\sigma_{y_0}(\tau = 5\,\text{days}) = 5.6 \times 10^{-15}$ and $t_{10}(\tau = 5\,\text{days}) = 18.9$ years.

If the performance trend of the last 25 years continues, in ten years, the UTC instability is expected to be 7.8×10^{-17} for $\tau = 5$ days. Similarly, $\sigma_{y_0}(\tau = 1\,\text{year}) = 1 \times 10^{-15}$ and $t_{10}(\tau = 1\,\text{year}) = 16.7$ years. Therefore, the instability of UTC could be reduced to 1.1×10^{-17} for $\tau = 1$ year in about a decade. It should be noted that to obtain these latter values, it is necessary to use datasets of at least three years in the computation of the dynamic Allan deviation. Fig. 7 shows

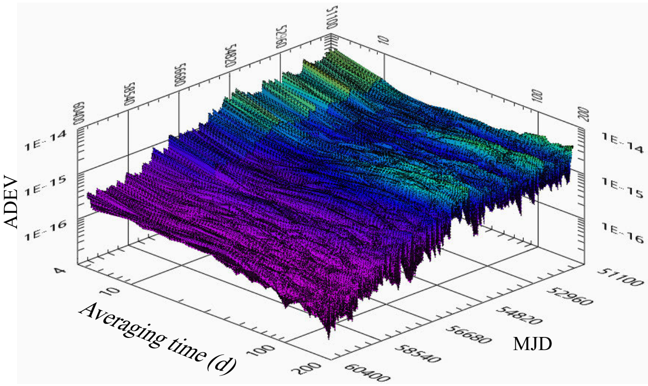

Fig. 6. Graph of the simple average dynamic Allan deviation of UTC.

simple average dynamic Allan deviation of UTC for $\tau = 5$ days and $\tau = 1$ year, as well as their respective fittings using (5).

It is pertinent to make some comments on the results shown. The UTC–UTC(k) measurements include noise due to the different time transfer links. It is not possible to assess the instability of each UTC(k) for averaging times less than five days, as there are no available data of continuous measurements, by other more direct means, for all laboratories and during the period analyzed (25 years).

In applying the three-corner hat method, it is strictly necessary to satisfy the condition of statistical independence, which requires having UTC–UTC(k_i), UTC–UTC(k_j), and UTC(k_i)–UTC(k_j) measurements obtained independently. However, even under ideal conditions, there will always be some level of correlation between UTC and UTC(k), as the primary goal of laboratories is to keep UTC–UTC(k) as close to zero as possible. This study represents an effort to estimate the simple and weighted average dynamic Allan deviation of UTC using the available data.

To evaluate our results, we computed the dynamic Allan deviation using the frequency difference (d) between PFS/SFS and TAI [74] (Fig. 8). The d values can be considered reliable to compute the instability of TAI for $\tau = 30$ days [3]. Fig. 8 also shows results presented in this article for UTC instability for $\tau = 30$ days. As can be seen in that figure, our results are in good agreement with those for TAI. In particular, both results have the same slope in the last 18 years as the simple average. A systematic difference by a factor of three can also be observed between the two graphs, associated with the noise differences between the time transfer links used.

To increase the confidence in our results presented in Figs. 6–8, we computed the average dynamic Allan deviation (simple and weighted) of UTC using data from all 10 UTC(k) laboratories discussed in Section II. For the weighted dynamic Allan deviation of UTC, we used weights defined by the relation $\omega_{y_{\mathrm{UTC}}} = (1/\sigma^2_{y_{\mathrm{UTC},i}})/(\sum_{i=1}^{N} 1/\sigma^2_{y_{\mathrm{UTC},i}})$, where $\sigma_{y_{\mathrm{UTC},i}}$ represents the Allan variance of the ith laboratory. Results of the average dynamic Allan deviation (simple and weighted) of UTC using all 10 UTC(k) laboratories are presented in Fig. 9.

We found that the UTC instability decreasing rates (time required to decrease instability by one order of magnitude) are 23.7 and 29.9 years, respectively. In contrast, the instability

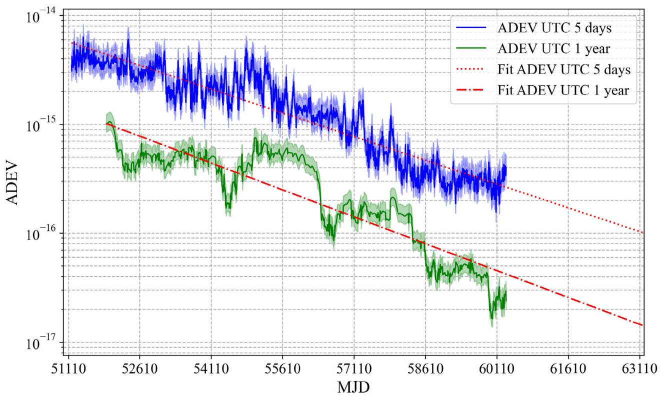

Fig. 7. Graph of the simple average dynamic Allan deviation of UTC for $\tau = 5$ days (blue), $\tau = 1$ year (green), and the corresponding fits in red (dotted for $\tau = 5$ days and dashed-dotted for $\tau = 1$ year) represent fittings using (5), while the shaded areas represent the confidence intervals.

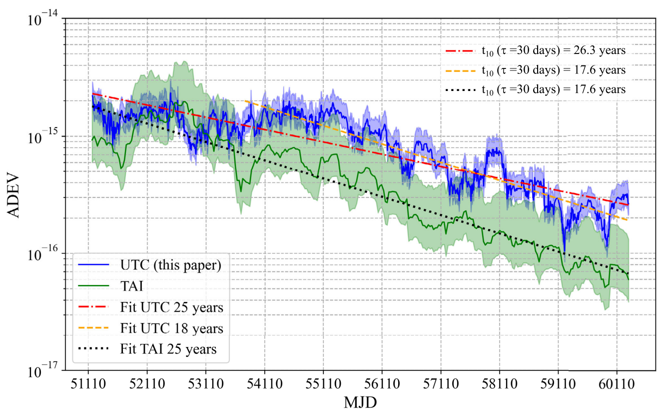

Fig. 8. Graph shows the simple average dynamic Allan deviation of the frequency difference (d) between PFS/SFS and TAI (green) and UTC for $\tau = 30$ days (blue) using 5 UTC(k) laboratories selected to calculate data included in Fig. 6. The red dashed-dotted line is the fit over the entire data, while the orange dashed line is the fit over the past 18 years, both for UTC and the black dotted line is the fit over the past 25 years for TAI. The shaded areas represent the calculation confidence intervals.

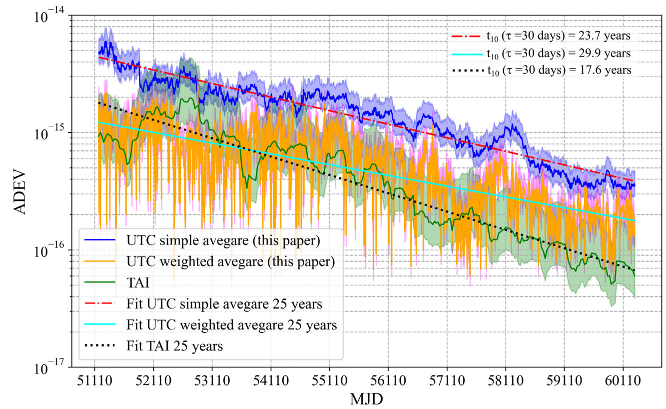

Fig. 9. Graph shows the average dynamic Allan deviation (simple and weighted in blue and orange, respectively) of the frequency difference (d) between PFS/SFS and TAI (green) and UTC for $\tau = 30$ days (blue) using all 10 UTC(k) laboratories presented in Section II. The red dashed-dotted line and the cyan line represent the fits over the entire dataset using the simple and weighted averages, respectively. The black dotted line represents the fit over the past 25 years for TAI. The shaded areas indicate the confidence intervals of the calculations.

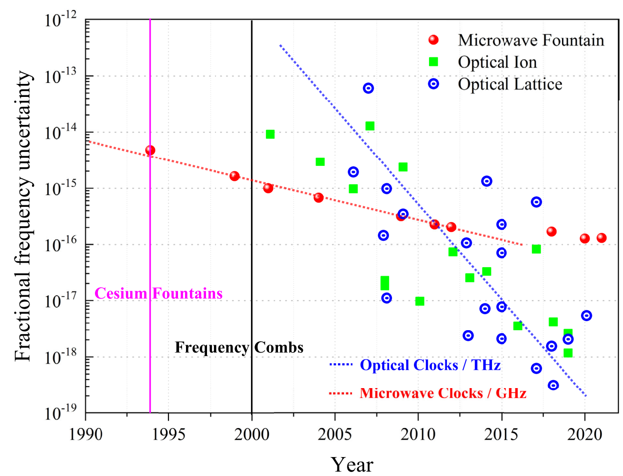

Fig. 10. Progress of the last 25 years of the microwave and optical clocks fractional frequency uncertainty.

decreasing rate when using data from the five best laboratories (those with the most stable UTC(k) timescales and fewer negative variance values) in a simple average scheme is 26.3 years. As observed, the instability decreasing rate when using data from the five best laboratories in a simple average scheme falls between the values obtained when data from all 10 laboratories are used (with a simple average and a weighted average). This outcome is expected, as using a simple average with data from all ten laboratories allows those with larger instability values to dominate the result. However, when data from those ten labs are used in a weighted average scheme, laboratories with smaller instability values tend to dominate the result. In summary, using the data from the most stable UTC(k) laboratories in a simple average scheme provides a good estimation of UTC stability.

The graph in Fig. 10 shows the progress in microwave clocks over the last 25 years [75], [76], [77]. Their fractional frequency uncertainty has decreased by an order of magnitude in about 17 years, which is consistent with the results presented here.

IV. Conclusion

The UTC and UTC(k) timescales are paramount for science, technology, economy, and safety. So far, UTC has been calculated for more than a half-century; it has been calculated by the BIPM since 1988, and before that by its predecessor, the International Time Bureau (BIH), since the early 1970s. The evolution of UTC and the UTC(k) timescales has been closely related to advances in science and technology. During the last 25 years, contributions of cold atom frequency standards and optical frequency standards have been included in the calculation of TAI and UTC, as well as in the computation of some UTC(k) timescales. Advances in time and frequency time transfer techniques also improve UTC computation.

Our analysis of the performance of UTC and some UTC(k) timescales during the last estimates of 25 years has found that their instability has decreased by about one order of magnitude in periods of about 19 years where $\tau = 5$ days and 17 years where $\tau = 1$ year. This rate of improvement can be exceeded in future years if fully hybrid UTC(k) timescales are developed that take advantage of an optical re-definition of the SI second.

REFERENCES

[1] H. Barrell, “Thirteenth general conference of weights and measures,” *Phys. Bull.*, vol. 20, pp. 61–62, Nov. 1969.

[2] D. B. Newell and E. Tiesinga, Eds., *The International System of Units (SI)*, document NIST Special Publication 330, 2019.

[3] G. Panfilo and F. Arias, “The coordinated universal time (UTC),” *Metrologia*, vol. 56, no. 4, Jun. 2019, Art. no. 042001.

[4] J. M. López-Romero and C. A. Ortiz-Cardona, “Atomic timescales,” in *Handbook of Metrology and Applications*. Heidelberg, Germany: Springer, Jan. 2023, pp. 409–430.

[5] D. D. McCarthy, “Evolution of timescales from astronomy to physical metrology,” *Metrologia*, vol. 48, no. 4, pp. S132–S144, Aug. 2011.

[6] R. L. Beard, “Role of the ITU-R in time scale definition and dissemination,” *Metrologia*, vol. 48, no. 4, pp. S125–S131, Aug. 2011.

[7] E. F. Arias and G. Petit, “The hyperfine transition for the definition of the second,” *Annalen der Physik*, vol. 531, no. 5, May 2019, Art. no. 1900068.

[8] D. Wang, M. Li, X. Huang, and X. Zhang, *Spacecraft Autonomous Navigation Technologies Based on Multi-Source Information Fusion*. Cham, Switzerland: Springer, 2021.

[9] BIPM. *Circular T*. ISSN 1143-1393. Accessed: Mar. 9, 2023. [Online]. Available: https://www.bipm.org/en/time-ftp/circular-t

[10] *Measurement Comparisons in the CIPM MRA: Guidelines for Organizing, Participating and Reporting*, document CIPM MRA-G-11, ver. 1.1, BIPM, Jan. 2021.

[11] M. Kühne, A. Henson, C. Thomas, and Ö. Altan, “The CIPM MRA,” *Proc. Int. School Phys. 'Enrico Fermi'*, vol. 185, pp. 29–44, Jan. 2013.

[12] BIPM. *CCTF-K001.UTC*. Accessed: Nov. 10, 2024. [Online]. Available: https://www.bipm.org/kcdb/comparison?id=735

[13] H. Li, L. Han, R. Duan, and G. M. Garner, “Analysis of the synchronization requirements of 5G and corresponding solutions,” *IEEE Commun. Standards Mag.*, vol. 1, no. 1, pp. 52–58, Mar. 2017.

[14] Y. Qian, D. Wu, W. Bao, and P. Lorenz, “The Internet of Things for smart cities: Technologies and applications,” *IEEE Netw.*, vol. 33, no. 2, pp. 4–5, Mar. 2019.

[15] P. Tavella and G. Petit, “Precise time scales and navigation systems: Mutual benefits of timekeeping and positioning,” *Satell. Navigat.*, vol. 1, no. 1, pp. 1–12, Mar. 2020.

[16] G. Giorgi et al., “Advanced technologies for satellite navigation and geodesy,” *Adv. Space Res.*, vol. 64, no. 6, pp. 1256–1273, Jun. 2019.

[17] E. Dalkıran, T. Önel, O. Topçu, and K. A. Demir, “Automated integration of real-time and non-real-time defense systems,” *Defence Technol.*, vol. 17, no. 2, pp. 657–670, Apr. 2021.

[18] M. A. Weiss, G. Petit, and Z. Jiang, “A comparison of GPS common-view time transfer to all-in-view,” in *Proc. IEEE Int. Freq. Control Symp. Expo.*, Aug. 2005, pp. 324–328.

[19] P. Banerjee and D. Matsakis, *An Introduction to Modern Timekeeping and Time Transfer: GNSS Techniques for Time Transfer*. Cham, Switzerland: Springer, 2023.

[20] D. Kirchner, “Two-way time transfer via communication satellites,” *Proc. IEEE*, vol. 79, no. 7, pp. 983–990, Jul. 1991.

[21] W. Wang et al., “An improved protocol for performing two-way satellite time and frequency transfer using a satellite in an inclined geo-synchronous orbit,” *IEEE Trans. Ultrason., Ferroelectr., Freq. Control*, vol. 65, no. 8, pp. 1475–1486, Aug. 2018.

[22] R. Lichtenecker, “Terrestrial time signal dissemination,” *Real-Time Syst.*, vol. 12, pp. 41–61, Jan. 1997.

[23] M. Weiss, L. Cosart, J. Hanssen, and J. Yao, “Precision time transfer using IEEE 1588 over OTN through a commercial optical telecommunications network,” in *Proc. IEEE Int. Symp. Precis. Clock Synchronization Meas., Control, Commun. (ISPCS)*, Sep. 2016, pp. 1–5.

[24] W. Alghamdi and M. Schukat, “A security enhancement of the precision time protocol using a trusted supervisor node,” *Sensors*, vol. 22, no. 10, p. 3671, May 2022.

[25] D. L. Mills, “Internet time synchronization: The network time protocol,” *IEEE Trans. Commun.*, vol. 39, no. 10, pp. 1482–1493, Oct. 1991.

[26] H. Kopetz and W. Steiner, *Real-Time Systems: Design Principles for Distributed Embedded Applications: Real-Time Communication*. Cham, Switzerland: Springer, 2022.

[27] J. Levine and T. Parker, “The algorithm used to realize UTC(NIST),” in *Proc. IEEE Int. Freq. Control Symp. PDA Exhib.*, May 2002, pp. 537–542.

[28] J. Levine, “The UT1 and UTC time services provided by the National Institute of Standards and Technology,” in *The Science of Time 2016: Time in Astronomy & Society, Past, Present and Future*. Cham, Switzerland: Springer, 2017, pp. 127–139.

[29] G. W. Hoth, B. Patla, N. Ashby, and V. Gerginov, “Initial study of the distributed cavity phase shift for the new microwave cavities of cs fountains at NIST,” in *Proc. Joint Conf. Eur. Freq. Time Forum IEEE Int. Freq. Control Symp. (EFTF/IFCS)*, Apr. 2022, pp. 1–4.

[30] G. W. Hoth, J. A. Sherman, A. G. Radnaev, P. Mitchell, and V. Gerginov, “NIST-F3, a cesium fountain frequency reference,” in *Proc. Precise Time Time Interval Syst. Appl. Meeting*, Feb. 2023, pp. 183–188.

[31] S. R. Jefferts et al., “Accuracy evaluation of NIST-F1,” *Metrologia*, vol. 39, no. 4, pp. 321–336, Aug. 2002.

[32] T. P. Heavner, S. R. Jefferts, E. A. Donley, J. H. Shirley, and T. E. Parker, “NIST-f1: Recent improvements and accuracy evaluations,” *Metrologia*, vol. 42, no. 5, pp. 411–422, Oct. 2005.

[33] M. A. Lombardi, T. P. Heavner, and S. R. Jefferts, “NIST primary frequency standards and the realization of the Si second,” *NCSLI Measure*, vol. 2, no. 4, pp. 74–89, Dec. 2007.

[34] T. P. Heavner et al., “First accuracy evaluation of NIST-F2,” *Metrologia*, vol. 51, no. 3, pp. 174–182, Jun. 2014.

[35] K. Gibble, “Corrigendum: Comment on ‘first accuracy evaluation of NIST-F2,”’ *Metrologia*, vol. 53, no. 3, p. 1009, Jun. 2016.

[36] J. A. Sherman et al., *A Resilient Architecture for the Realization and Distribution of Coordinated Universal Time to Critical Infrastructure Systems in the United States: Methodologies and Recommendations From the National Institute of Standards and Technology (NIST)*, document NIST Technical Note 2187, 177, 2021.

[37] A. Bauch, S. Weyers, D. Piester, E. Staliuniene, and W. Yang, “Generation of UTC (PTB) as a fountain-clock based time scale,” *Metrologia*, vol. 49, pp. 1–34, Jan. 2012.

[38] D. Piester et al., “PTB's time and frequency services 2015–2016,” in *Proc. Precise Time Time Interval Syst. Appl. Meeting*, Mar. 2017, pp. 53–61.

[39] S. Weyers, U. H. bner, R. S. der, C. Tamm, and A. Bauch, “Uncertainty evaluation of the atomic caesium fountain CSF1 of the PTB,” *Metrologia*, vol. 38, no. 4, pp. 343–352, Aug. 2001.

[40] S. Weyers, A. Bauch, R. Schröder, and C. Tamm, “The atomic caesium fountain CSF1 OF PTB,” in *Proc. 6th Symp. Freq. Standards Metrol.*, vol. 5, May 2002, pp. 64–71.

[41] R. Wynands, D. Griebsch, R. Schröder, and S. Weyers, “Current status of PTB's new caesium fountain clock CSF2,” in *Proc. 20th Eur. Freq. Time Forum*, Mar. 2006, pp. 200–202.

[42] V. Gerginov, N. Nemitz, S. Weyers, R. Schröder, D. Griebsch, and R. Wynands, “Uncertainty evaluation of the caesium fountain clock PTB-CSF2,” *Metrologia*, vol. 47, no. 1, pp. 65–79, Feb. 2010.

[43] A. Clairon, P. Laurent, G. Santarelli, S. Ghezali, S. N. Lea, and M. Bahoura, “A cesium fountain frequency standard: Preliminary results,” *IEEE Trans. Instrum. Meas.*, vol. 44, no. 2, pp. 128–131, Apr. 1995.

[44] P. Laurent et al., “A cold atom clock in absence of gravity,” *Eur. Phys. J. D*, vol. 3, no. 3, p. 201, 1998.

[45] J. Guena et al., “Demonstration of a dual alkali Rb/Cs fountain clock,” *IEEE Trans. Ultrason., Ferroelectr., Freq. Control*, vol. 57, no. 3, pp. 647–653, Mar. 2010.

[46] G. D. Rovera et al., “UTC(OP) based on LNE-SYRTE atomic fountain primary frequency standards,” *Metrologia*, vol. 53, no. 3, pp. S81–S88, Jun. 2016.

[47] F. J. Galindo, “CCTF 2009: Report of the real observatorio de la armada,” Real Observatorio de la Armada, Sevres, France, Tech. Rep. 18, 2009.

[48] *Real Observatorio De La Armada*. Accessed: Oct. 30, 2023. [Online]. Available: https://n9.cl/xkw79

[49] K. Szymaniec, W. Chalupczak, D. Henderson, and Y. Ovchinnikov, “Evaluation of NPL CSF1 primary frequency standard,” in *Proc. Conf. Precis. Electromagn. Meas.*, Jun. 2004, pp. 496–497.

[50] K. Szymaniec, W. Chalupczak, P. B. Whibberley, S. N. Lea, and D. Henderson, “Evaluation of the primary frequency standard NPL-CsF1,” *Metrologia*, vol. 42, no. 1, pp. 49–57, Feb. 2005.

[51] K. Szymaniec, S. E. Park, G. Marra, and W. Chałupczak, “First accuracy evaluation of the NPL-CsF2 primary frequency standard,” *Metrologia*, vol. 47, no. 4, pp. 363–376, Aug. 2010.

[52] K. Szymaniec and S. E. Park, “Primary frequency standard NPL-CsF2: Optimized operation near the collisional shift cancellation point,” *IEEE Trans. Instrum. Meas.*, vol. 60, no. 7, pp. 2475–2481, Jul. 2011.

[53] K. Szymaniec, S. N. Lea, K. Gibble, S. E. Park, K. Liu, and P. Głowacki, "NPL Cs fountain frequency standards and the quest for the ultimate accuracy," *J. Phys., Conf. Ser.*, vol. 723, Jun. 2016, Art. no. 012003.

[54] P. Whibberley, E. L. English, C. Langham, K. Szymaniec, and R. Hendricks, "Improvement of the UTC(NPL) time scale recent upgrades and future plans," in *Proc. Joint Conf. IEEE Int. Freq. Control Symp. Eur. Freq. Time Forum (EFTF/IFC)*, Apr. 2019, pp. 1–2.

[55] S. W. Lee, C. B. Lee, and S. H. Yang, "A new approach for steering UTC (KRIS)," *IEEE Trans. Instrum. Meas.*, vol. 58, pp. 1247–1251, 2008.

[56] F. Cordara, R. Costa, and V. Pettiti, "Generation of the national time scale UTC (IT) at INRIM: An update," in *Proc. Eur. Freq. Time Forum*, Apr. 2008, pp. 1–7.

[57] G. Signorile et al., "Preliminary step for a UTC(IT) steering algorithm based on the ITCsF2 primary frequency standard measurements," in *Proc. Joint Conf. IEEE Int. Freq. Control Symp. Eur. Freq. Time Forum*, Apr. 2015, pp. 260–264.

[58] L. Galleani, G. Signorile, V. Formichella, and I. Sesia, "Generating a real-time time scale making full use of the available frequency standards," *Metrologia*, vol. 57, no. 6, Dec. 2020, Art. no. 065015.

[59] F. Levi, D. Calonico, C. E. Calosso, A. Godone, S. Micalizio, and G. A. Costanzo, "Accuracy evaluation of ITCsF2: A nitrogen cooled caesium fountain," *Metrologia*, vol. 51, no. 3, pp. 270–284, Jun. 2014.

[60] S. R. Jefferts et al., "High-accuracy measurement of the blackbody radiation frequency shift of the ground-state hyperfine transition in ^{133}Cs," *Phys. Rev. Lett.*, vol. 112, no. 5, Feb. 2014, Art. no. 050801.

[61] F. Levi, L. Lorini, D. Calonico, and A. Godone, "Systematic shift uncertainty evaluation of IEN CSF1 primary frequency standard," *IEEE Trans. Instrum. Meas.*, vol. 52, no. 2, pp. 267–271, Apr. 2003.

[62] J. M. López-Romero, M. A. Lombardi, N. Diaz-Muñoz, and E. de Carlos-Lopez, "SIM time scale," *IEEE Trans. Instrum. Meas.*, vol. 62, no. 12, pp. 3343–3350, Dec. 2013.

[63] J. M. López-Romero and N. Díaz-Muñoz, "Progress in the generation of the UTC(CNM) in terms of a virtual clock," *Metrologia*, vol. 45, no. 6, pp. S59–S65, Dec. 2008.

[64] F. Roosbeek, P. Defraigne, and A. Somerhausen, "Setting up an NTP server at the royal observatory of Belgium," in *Proc. 36th Annu. Precise Time Time Interval Syst. Appl. Meeting*, 2004, pp. 237–246.

[65] K. A. Van der Hucht and A. Karel, "Commission 31: Time," in *Proc. Rep. Astron. (IAU XXVIIA): IAU Trans. XXVIIA*, vol. 27, 2009, pp. 50–54.

[66] Real Observatory of Belgium. *Realization of UTC(ORB)*. Accessed: Sep. 18, 2023. [Online]. Available: https://betime.be/en/missions/UTC-ORB.php

[67] D. Matsakis, "Time and frequency activities at the U.S. Naval Observatory," in *Proc. IEEE Int. Freq. Control Symp. Exposit.*, Aug. 2005, pp. 217–224.

[68] G. Petit, F. Arias, A. Harmegnies, G. Panfilo, and L. Tisserand, "UTCr: A rapid realization of UTC," *Metrologia*, vol. 51, no. 1, pp. 33–39, Feb. 2014.

[69] L. Galleani and P. Tavella, "The dynamic Allan variance," *IEEE Trans. Ultrason., Ferroelectr., Freq. Control*, vol. 56, no. 3, pp. 450–464, Mar. 2009.

[70] G. Panfilo, A. Harmegnies, and L. Tisserand, "A new weighting procedure for UTC," *Metrologia*, vol. 51, no. 3, pp. 285–292, Jun. 2014.

[71] G. Panfilo, A. Harmegnies, and L. Tisserand, "A new prediction algorithm for the generation of international atomic time," *Metrologia*, vol. 49, no. 1, pp. 49–56, Feb. 2012.

[72] N. Dimarcq et al., "Roadmap towards the redefinition of the second," *Metrologia*, vol. 61, no. 1, Dec. 2023, Art. no. 012001.

[73] T. E. Parker, "Three-corner-hat analysis of the stability of UTC and various UTC (K)'s," in *Proc. 45th Annu. Precise Time Time Interval Syst. Appl. Meeting*, 2013, pp. 269–273.

[74] BIPM. *Estimate of d By the BIPM Based on All PSFS Measurements Identified to Be Used for TAI Steering*. Accessed: Dec. 6, 2024. [Online]. Available: https://webtai.bipm.org/ftp/pub/tai/other-products/taipsfs/fpsfs-ftai

[75] L. Sharma et al., "Optical atomic clocks for redefining Si units of time and frequency," *MAPAN*, vol. 35, no. 4, pp. 531–545, Dec. 2020.

[76] I. Alonso et al., "Cold atoms in space: Community workshop summary and proposed road-map," *EPJ Quantum Technol.*, vol. 9, no. 1, pp. 1–55, Nov. 2022.

[77] E. Boldbaatar, D. Grant, S. Choy, S. Zaminpardaz, and L. Holden, "Evaluating optical clock performance for GNSS positioning," *Sensors*, vol. 23, no. 13, p. 5998, Jun. 2023.

C. A. Ortiz received the B.E. degree in electronic engineering from the University of Quindío, Armenia, Colombia, in 2004, the M.Sc. degree in science and materials engineering from the National Autonomous University of Mexico (UNAM), Mexico City, Mexico, in 2012, and the Ph.D. degree in science (materials) from the Center for Research and Advanced Studies, National Polytechnic Institute (CINVESTAV), Mexico City, in 2018.

Since 2017, he has been a Scientific Coordinator with the Time and Frequency Division, National Center of Metrology (CENAM), El Marqués, Mexico. His current research interests include timescale generation, primary frequency standards, quantum optics, synchrony for telecommunications, and atomic physics.

Dr. Ortiz is a member of the Consultative Committee for the Time and Frequency Working Group on TAI (CCTF-WGTAI) and the International Bureau of Weights and Measures (BIPM).

E. de Carlos-López received the Ph.D. degree in physics from the Universidad Autónoma del Estado de Morelos, Cuernavaca, Mexico, in 2008.

He joined the Time and Frequency Division, Centro Nacional de Metrología, El Marqués, Mexico, in 2008. He has participated actively in the development of the SIM time and frequency comparison network and the SIM timescale. His current research interests include cold atoms physics, primary frequency standards, cesium fountain clocks, optical frequencies, and timescales.

A. Medina-Herrera received the Ph.D. degree in science (materials) from the Center for Research and Advanced Studies, National Polytechnic Institute (CINVESTAV), Santiago de Querétaro, Mexico, in 2023.

In 2022, he worked with the Electromagnetism Division at the Centro Nacional de Metrología, El Marqués, Mexico. He is currently a Postdoctoral Researcher at the Physikalisch-Technische Bundesanstalt (PTB), 8.22 Metrology of Ultralow Magnetic Fields, Berlin, Germany. His current research interests include comagnetometers, ultralow magnetic fields, cold atom physics, atomic physics, and optical frequencies.

Michael A. Lombardi (Member, IEEE) is a Research Associate with the Time and Frequency Division, National Institute of Standards and Technology (NIST), Boulder, CO, USA. He was a full-time Staff Member of the division from 1981 to 2023. From 2019 to 2023, he was the Leader of the Time Realization and Distribution Group. He has authored or co-authored more than 100 papers related to frequency and time metrology.

Lombardi was a recipient of a NIST Distinguished Career Award.

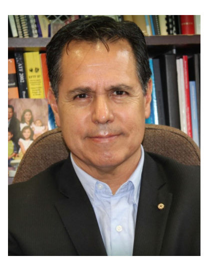

J. M. López-Romero (Member, IEEE) received the Ph.D. degree in physics from the Centro de Investigacion y Estudios Avanzados del IPN (CINVESTAV-IPN), Mexico City, Mexico, in 1993.

In 1994, he joined the Centro Nacional de Metrología (CENAM), El Marqués, Mexico, as the Chief of the Time and Frequency Division. In 2015, he joined CINVESTAV, as the Director of CINVESTAV Campus Querétaro. He was Chair of the SIM Time and Frequency Working Group. He has participated actively in the development of the SIM time and frequency comparison network and the SIM timescale. His current research interests include timescale generation, primary frequency standards, cesium fountain clocks, quantum gravimeters, optical frequencies, and quantum cryptography.